Communications in Physics, Vol. 33, No. 4 (2023), pp. 343-354
DOI: https://doi.org/10.15625/0868-3166/18660

Measurement of the flux-weighted average cross section for the $^{186}W(\gamma, p)^{185}Ta$ reaction at the bremsstrahlung end-point energy of 70 MeV

Nguyen Van Do[1,2,†], **Tran Dinh Trong**[3], **Kim Tien Thanh**[3], **Nguyen Thi Hien**[4], **Guinyun Kim**[4] **and Bui Thi Hoa**[5]

[1]*Institute of Theoretical and Applied Research, Duy Tan University, Hanoi 100000, Vietnam*

[2]*Faculty of Natural Sciences, Duy Tan University, Da Nang 550000, Vietnam*

[3]*Institute of Physics, Vietnam Academy of Science and Technology, 10 Dao Tan, Ba Dinh, Hanoi 11108, Vietnam*

[4]*Department of Physics, Kyungpook National University, Daegu 415661, Republic of Korea*

[5]*VNU University of Science, Vietnam National University, 334 Nguyen Trai Str., Hanoi, Vietnam*

E-mail: [†]ngvando2404@gmail.com

Received 17 August 2023
Accepted for publication 30 September 2023
Published 21 December 2023

Abstract. *The flux-weighted average cross section for the $^{186}W(\gamma, p)^{185}Ta$ reaction induced with 70 MeV bremsstrahlung end-point energy was measured using the activation method in combination with off-line gamma activity measurement. The $^{27}Al(\gamma,2pn)^{24}Na$ monitor reaction was used for the determination of the bremsstrahlung flux. The bremsstrahlung photons used to produce the photonuclear reactions were generated from a thin tungsten (W) converter by bombardment with a 70 MeV electron beam. The experimental flux-weighted average cross section is compared with the theoretical prediction, for which the absolute cross section was calculated using the TALYS 1.95 code and the bremsstrahlung spectrum was simulated using the computer program MCNPX. The present experiment was carried out at the 100 MeV electron linac of the Pohang Accelerator Laboratory, POSTECH, Pohang, Korea.*

Keywords: $^{186}W(\gamma, p)^{185}Ta$ reaction; averaged cross-section; bremsstrahlung end-point energy of 70 MeV; activation and off-line γ-ray spectrometry; TALYS1.95; MCNPX.

Classification numbers: 25.20.-x; 29.30.Kv.

1. Introduction

Photonuclear reactions play an important role in various aspects of basic nuclear physics research and in different fields of application [1, 2]. In recent decades, both the well-developed electron linacs capable of generating bremsstrahlung photons with energies of tens or more than tens of MeV and the high-quality γ-ray measuring instruments have offered advantages for research on photonuclear reactions. The high-energy photons are able to produce nuclear reactions with a variety of complexity by emitting not only a single nucleon such as (γ,n) [3–6] or (γ,p) [6–8], but also multi-particle emission reactions such as (γ,xn) [9, 10] or (γ,xnyp) with $x,y \geq 1$ [11].

The complexity of the nuclear reactions increases as the energy of incident bremsstrahlung photons increases. At relatively low energies of incident photons, in the range ≤ 30 MeV, the so-called giant dipole resonance (GDR) energy region, photonuclear reactions occur mainly due to a compound mechanism. However, at higher incident energies, nuclear reactions can also be processed via additional mechanisms such as pre-equilibrium and direct. This is also another important reason for studying nuclear reactions with increasing incident energies.

In this work, we chose the $^{186}W(\gamma,p)^{185}Ta$ reaction for study with an incident bremsstrahlung end-point energy of 70 MeV, beyond the GDR energy range. As it is known, W is a potential structural material of a fusion reactor, so the knowledge of the cross section of nuclear reactions on W is necessary. The $^{186}W(\gamma,p)^{185}Ta$ reaction produces a neutron-rich ^{185}Ta isotope, which was first observed by Butement in 1950 through the $^{186}W(\gamma,p)$ photonuclear reaction by 23 MeV X-rays from the synchrotron [12]. However, no literature data for the $^{186}W(\gamma,p)^{185}Ta$ reaction were found. Although we found some reports in the literature about the production of ^{185}Ta from ^{186}W, but those were not by the (γ,p) reaction. Shizuma et al reported the studies on the production of ^{185}Ta through the one-proton acceptance reaction $^{186}W(^{18}O,^{19}F)^{185}Ta$ [13], Li et al measured cross section of the $^{186}W(n,d)^{185}Ta$ reaction around 14 MeV neutrons [14], Lovhoiden et al studied the $^{186}W(t,\alpha)^{185}Ta$ reaction using 17 MeV tritons [15], Semkova et al studied the cross section of the $^{186}W(n,x)^{185}Ta$ reaction with energies between 13.5 and 20.6 MeV [16], and Sakane et al reported the studies on the cross section of the $^{186}W(n,n'p)^{185}Ta$ reaction by 14 MeV neutron [17].

The present study focuses on measurements of the flux-weighted average cross section of the $^{186}W(\gamma,p)^{185}Ta$ reaction induced with a bremsstrahlung end-point energy of 70 MeV. Since the ^{185}Ta radionuclide has gamma rays and a half-life suitable for the activity measurement, the experiment was performed using the well-known activation method in combination with off-line gamma spectrometry [18–20]. Due to the lack of experimental data, the present result is compared to the theoretical prediction, using the TALYS 1.95 code [21]. For the calculations, the effect of the nuclear level density was taken into account by considering six level density models.

2. Experiment

This experimental procedure contains three main steps, (1) irradiation of the sample to convert the stable target nuclides into radioactive isotopes, (2) measurement of the activity of the radionuclides produced, and (3) data analysis to derive the flux-weighted average cross section of the $^{186}W(\gamma,p)^{185}Ta$ reaction.

2.1. *Irradiation of the sample*

Natural tungsten foil (W) with a purity of 99.95%, a size of 12 mm ×12 mm and a thickness of 0.1 mm was prepared for the irradiation at the electron accelerator of the Pohang Accelerator Laboratory, POSTECH, Pohang, Korea. In the present experiment, the bremsstrahlung flux was monitored by the ^{27}Al(γ,2np)^{24}Na reaction. For this purpose, the aluminum foil of 99% purity with the same dimension as W sample was also prepared and the stack of Al-W foils was irradiated simultaneously. The bremsstrahlung photon beam with the maximum energy of 70 MeV was generated by bombarding a 70 MeV electron beam into the thin W converter with a size of 100 x 100 mm and a thickness of 0.1 mm. The geometric arrangement for the irradiation was the same as in our previous experiment [11], namely the tungsten converter was placed 15 cm from the electron exit window and the stack of Al-W foils was placed 12 cm from the tungsten converter. During irradiation, the intensity of the electron beam was fixed at 50 mA, the pulse width of the electron beam was 1.2 μs, the repetition frequency was 15 Hz, and the irradiation time was 60 min. The nuclear reactions of interest in this study are ^{186}W$(\gamma, p)^{185}$Ta and ^{27}Al(γ,2pn)^{24}Na, and the main decay data of the residual nuclei are listed in Table 1 [22].

Table 1. Investigated nuclear reactions and main decay data of the reaction products ^{185}Ta and ^{24}Na 22.

Nuclearreaction	E_{thr} (MeV)	$T_{1/2}$	Decay mode (%)	Spin	E_γ (keV)	I_γ (%)
^{186}W$(\gamma, p)^{185}$Ta	8.40	49.4 m	β^-: 100	7/2$^+$	107.80	2.75
					173.91*	22.6
					177.59*	25.7
					243.70	3.8
^{27}Al(γ,2pn)^{24}Na	31.45	14.997 h	β^-: 100	4$^+$	1368.62*	99.99
					2754.0	99.85

* *γ-ray used for activity measurement.*

2.2. *Activity measurement*

The γ-spectra of both the irradiated W sample and the Al monitor were measured off-line by the HPGe γ-ray detector (ORTEC, GEM-2018-p) connected to a PC-based 4K channel analyzer. The energy resolution of the HPGe detector is 1.8 keV at the γ-peak of 1332.5 keV from ^{60}Co. The detection efficiency of the detector at 1332.5 keV is 20% relative to that of the 76 mm × 76 mm NaI(Tl) detector. The efficiency of the detector was calibrated at different distances from the detector surface using standard γ-sources as described elsewhere [23].

Considering the advantage of high activity of irradiated samples, the measurement was performed by placing the sample at 10 cm from the surface of the HPGe detector to reduce counting losses due to detector dead time and coincidence summing effect. Typical γ-ray spectra of the irradiated W foil sample and Aluminum monitor are shown in Fig. 1 and Fig. 2, respectively.

As can be seen in Fig. 1, the γ-ray spectrum of the W foil sample shows a number of photo peaks. However, the two γ-rays of 173.91 keV and 177.59 keV are suitable for the activity measurement of the ^{185}Ta radionuclide. The main reason for this choice was that none of the gamma

rays were interfered or overlapped with the γ-rays of 173.91 keV or 177.59 keV. In addition, both the 173.91 keV and 177.59 keV photopeaks have relatively good statistics, with a statistical uncertainty of about 1.5-2.0%. This makes the analysis of the γ-ray spectra easier and more accurate.

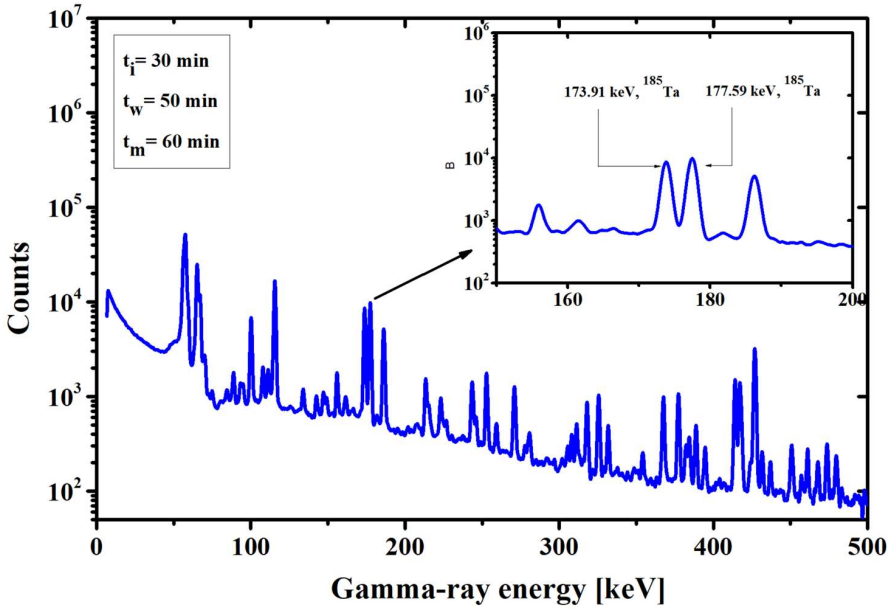

Fig. 1. Typical γ-ray spectrum of W foil sample irradiated with a bremsstrahlung end-point energy of 70 MeV. The irradiation, waiting, and measurement times were 30, 50, and 60 min, respectively. A part of the γ-ray spectrum in the upper right corner of this figure shows the main γ-peaks at 173.91 keV (22.6%) and 177.59 kev (25.7%) of the ^{185}Ta radionuclide, which are used for measuring activity.

The ^{24}Na radionuclide emits two gamma rays at 2754.0 keV (99.85%) and 1368.62 keV (99.99%). In principle, both γ-rays are of high intensity, which can be used for the measurement of ^{24}Na activity. In the present experiment, the 1368.62 keV (99.99%) γ-ray was chosen for the measurement, since its detection efficiency is higher than that of 2754.0 keV. Additionally, as shown in Fig. 2, the 1368.62 keV γ-ray is interference-free and appears in the relatively low background gamma spectrum.

The measured γ-ray spectra were processed using the computer program GammaVision, version 5.10 (EG&G, ORTEC), which was able to accurately determine the energy of the appearing γ-peaks and the number of counts under each photo peak considered in the γ-ray spectra.

2.3. Data analysis

The flux-weighted average cross section for a given photonuclear reaction, over an energy range from the reaction threshold to the bremsstrahlung end-point energy can be expressed as follows [19]:

$$\langle \sigma(E_{\gamma\max}) \rangle = \frac{\int_{E_{thr}}^{E_{\gamma\max}} \sigma(E)\phi(E)dE}{\int_{E_{thr}}^{E_{\gamma\max}} \phi(E)dE}, \quad (1)$$

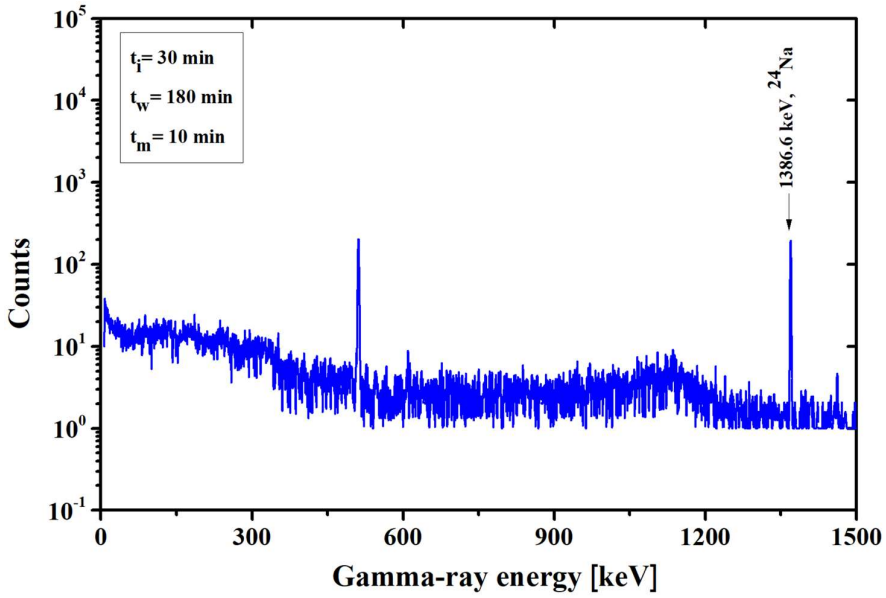

Fig. 2. Typical γ-ray spectrum of Aluminum foil sample irradiated with bremsstrahlung end-point energy of 70 MeV. The irradiation, waiting and measurement times were 30, 180, and 10 min, respectively.

where $\sigma(E)$ is the energy dependent cross section, $\Phi(E)$ is the bremsstrahlung flux at the given energy E, E_{thr} and $E_{\gamma\max}$ are the reaction threshold and bremsstrahlung end-point energies, respectively. The integral $\int_{E_{thr}}^{E_{\gamma\max}} \phi(E)dE$ gives the integrated bremsstrahlung flux in the energy range from the reaction threshold, E_{thr} to the bremsstrahlung end-point energy, $E_{\gamma\max}$, which is incident on W foil sample, resulting in the $^{186}\mathrm{W}(\gamma,p)^{185}\mathrm{Ta}$ reaction. The integrated bremsstrahlung flux for the studied reaction (x) is now denoted by $\phi_{\mathrm{int},x}$. So, the flux-weighted average cross section of the nuclear reaction expressed in Eq. (1) can be briefly rewritten as:

$$\langle\sigma(E_{\gamma\max})\rangle = \frac{Y_{Exp}(E_{\gamma\max})}{\phi_{\mathrm{int},x}}. \tag{2}$$

In order to obtain the flux-weighted average cross section, it is necessary to measure the reaction yield, $Y_{Exp}(E_{\gamma\max})$ and the integrated bremsstrahlung flux, $\phi_{\mathrm{int},x}$ incident on the target nuclide to form the nuclear reaction under study. By using the activation method in combination with off-line γ-ray spectrometry, the reaction yield can be obtained as follows:

$$Y_{Exp}(E_{\gamma\max}) = \frac{S_\gamma f\lambda(1-e^{-\lambda T})}{N_0 I_\gamma \varepsilon_\gamma (1-e^{-\lambda\tau})e^{-\lambda(T-\tau)}(1-e^{-\lambda t_i})e^{-\lambda t_w}(1-e^{-\lambda t_m})}, \tag{3}$$

where S_γ is the photo-peak area (or total number of counts) of the selected gamma ray of the residual nuclide, λ is the decay constant, f is the correction factor for the counting losses due to the self-absorption, which is calculated by the simple expression: $f = (1-e^{-\mu d})/\mu d$, where μ is the linear absorption coefficient and d is the sample thickness, I_γ is the intensity of γ-ray emitted

from the residual nuclide, ε_γ is the detector efficiency, which is determined experimentally as mentioned in subsection 2.2, τ is the pulse width of the electron beam and T is the cycle period, t_i, t_w, and t_m are the irradiation, waiting and measurement times.

The integrated bremsstrahlung flux incident on the aluminum target, resulting $^{27}Al(\gamma,2pn)^{24}Na$ monitor reaction, denoted by $\phi^{Exp}_{\text{int},mon}$, which represents the integrated bremsstrahlung flux over the threshold energy of 31.45 MeV to the end-point energy of 70 MeV can be obtained from the following expression:

$$\phi^{Exp}_{\text{int},mon} = \frac{S_{\gamma,mon} f \lambda (1-e^{-\lambda T})}{\langle \sigma^{Exp}_{mon} \rangle N_0 I_\gamma \varepsilon_\gamma (1-e^{-\lambda \tau}) e^{-\lambda (T-\tau)} (1-e^{-\lambda t_i}) e^{-\lambda t_w} (1-e^{-\lambda t_m})}, \tag{4}$$

where $S_{\gamma,mon}$ is the number of counts under the 1368.62 keV gamma-peak of ^{24}Na, $\langle \sigma^{Exp}_{mon} \rangle$ is the mean cross section of the monitor reaction $^{27}Al(\gamma,2pn)^{24}Na$ over the energy range from 31.45 MeV to the bremsstrahlung end-point energy of 70 MeV, and its value is 0.158 mb [19, 24], and all other terms have the same meaning as in Eq. (3).

As seen in Table 1, the threshold energy for the monitor reaction $^{27}Al(\gamma,2pn)^{24}Na$ is 31.45 MeV and that for the studied reaction $^{186}W(\gamma,p)^{185}Ta$ is 8.40 MeV. Thus, the integrated bremsstrahlung flux for the studied reaction

$$\int_{E_{thr,x}}^{E_{\gamma\max}} \phi(E)dE = \phi_{\text{int},x}$$

can be derived from that of the monitor reaction as follows:

$$\phi_{\text{int},x} = C_x \times \phi_{\text{int},mon}, \tag{5}$$

where $\phi_{\text{int},mon}$ is the integrated bremsstrahlung flux for the monitor reaction $^{27}Al\gamma,2pn)^{24}Na$ over the energy range from the threshold energy of 31.45 MeV to the end-point energy of 70 MeV, C_x is the conversion factor. As usual, the conversion factor can be obtained by calculation, taking into account the threshold energies of the two nuclear reactions, $^{186}W(\gamma,p)$ ^{185}Ta and $^{27}Al(\gamma,2pn)^{24}Na$ as follows [19]:

$$C_x = \int_{E_{thr,x}}^{E_{\gamma\max}} \phi(E)dE \Big/ \int_{E_{thr,mon}}^{E_{\gamma\max}} \phi(E)dE, \tag{6}$$

where $E_{th,x}$ and $E_{th,mon}$ are the threshold energy of the $^{186}W(\gamma,p)^{185}Ta$ and $^{27}Al(\gamma,2pn)^{24}Na$ reactions, respectively, $E_{\gamma\max}$ is the end-point energy of the bremsstrahlung spectrum and equals 70 MeV. The bremsstrahlung spectrum as a function of photon energy, $\phi(E)$ was obtained by simulation using MCNPX [25] computer program. The simulation took into account the actual arrangement of the experimental geometry, the dimension of the W target and the characteristics of the electron beam as described in subsection 2.1. The simulated bremsstrahlung spectrum is shown in Fig. 3. The conversion factor for the $^{186}W(\gamma,p)^{185}Ta$ reaction was calculated as $C_x = 3.19$. Finally, it was possible to determine the integrated bremsstrahlung flux for the $^{186}W(\gamma,p)^{185}Ta$ reaction according to the Eq. (5).

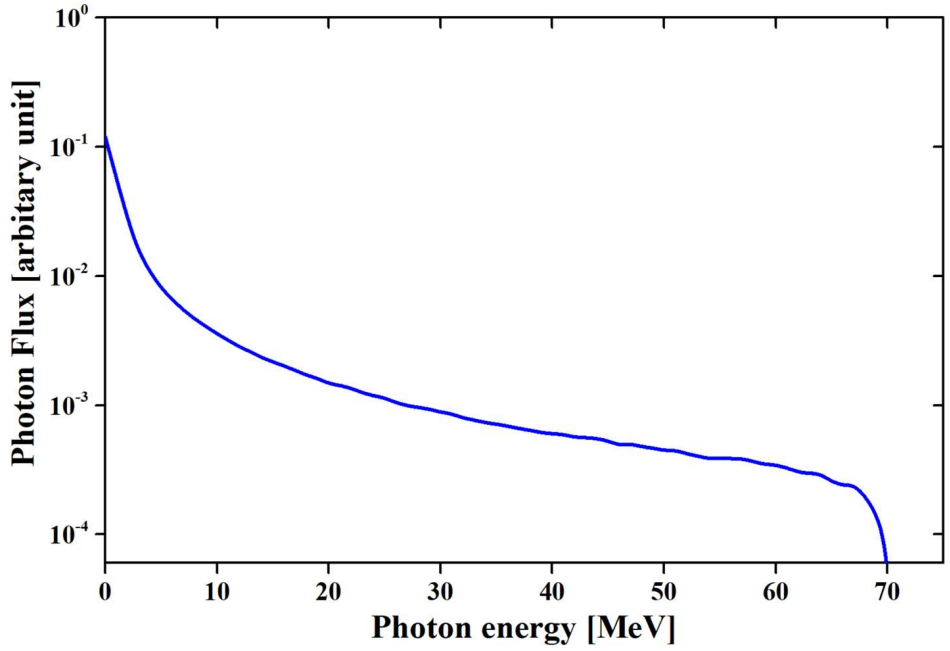

Fig. 3. The bremsstrahlung spectrum generated by impinging a 70 MeV electron beam on the W converter with a size of 100 mm × 100 mm and a thickness of 0.1 mm. The spectrum was simulated using the computer program MCNPX.

3. Results and discussion

3.1. Experimental result

The flux-weighted average cross section of the $^{186}\mathrm{W}(\gamma,p)^{185}\mathrm{Ta}$ reaction was determined from Eq. (2) based on the measured reaction yield, $Y_{Exp}(E_{\gamma\max})$ and the integrated bremsstrahlung flux, $\phi_{\mathrm{int},x}$. It should be noted that when determining the reaction yield, the contribution of the competing reaction $^{186}\mathrm{W}(n,x)^{185}\mathrm{Ta}$ was removed by slowing down the fast neutrons before entering the studied sample [26]. The flux-weighted average cross section of the $^{186}\mathrm{W}(\gamma,p)^{185}\mathrm{Ta}$ reaction induced with a bremsstrahlung end-point energy of 70 MeV obtained in this study is 0.105 ± 0.011 mb. The total uncertainty of the experimental result was determined according to the square root rule and gives values between 9 and 12%. The main sources of uncertainty included the statistical uncertainty (2 – 3%), the nuclear data used such as gamma intensity (4 – 5%) and half-life of the residual nuclide (3.1%), the detector efficiency (3 – 4%), the variation of the electron beam (5 – 6%) and the uncertainty expected from other sources (4 – 7%). In this experiment, by correcting for the gamma-ray self-absorption effect and avoiding the competing reaction $^{186}\mathrm{W}(n,d)^{185}\mathrm{Ta}$, the uncertainties caused by both become small and are included among the other sources of uncertainty.

Currently, no experimental data can be found in the literature regarding the flux-weighted average cross section of the $^{186}\mathrm{W}(\gamma,p)^{185}\mathrm{Ta}$ reaction. We therefore cannot compare the current results with the reference data. Instead, we compare the current result with theoretical predictions.

3.2. Model calculation results

We are unable to compare the current experimental result with others due to the lack of measurement data for the $^{186}W(\gamma,p)^{185}Ta$ nuclear reaction. In order to verify the present result, we calculate the flux-weighted average cross section of the $^{186}W(\gamma,p)^{185}Ta$ reaction for comparison. The flux-weighted average cross section was calculated according to Eq. (1). Accordingly, we need to calculate the reaction yield and the integral bremsstrahlung flux. The energy dependent cross section $\sigma(E)$ for the $^{186}W(\gamma,p)^{185}Ta$ reaction was calculated using the nuclear model code TALYS-1.95 [21]. The code TALYS was chosen for the calculation because it is user friendly, well documented and widely applied today. In addition, numerous nuclear models are available in the TALYS code that help simulate all possible nuclear reactions that occur with different projectiles such as γ-rays, protons, neutrons, deuterons, tritons, ^{3}He and ^{4}He with an incident energy between 1 keV and 200 MeV on nuclides with mass number between 12 and 339. The TALYS code also takes into account different reaction mechanisms, such as compound, pre-equilibrium and direct reactions, depending on the energy of the incident particles. The TALYS input is based on the RIPL-3 database (IAEA Reference Input Parameter Library) [27]. The total bremsstrahlung flux incident on the W foil sample, resulting in the $^{186}W(\gamma,p)^{185}Ta$ reaction was obtained by integrating $\int_{E_{thr}}^{E_{\gamma max}} \phi(E)dE$ over the energy range from the reaction threshold of $E_{thr} = 8.40$ MeV to the bremsstrahlung end-point energy of $E_{\gamma max} = 70$ MeV.

It is known that the nuclear level densities and gamma strength functions are the important ingredients to calculate the reaction cross section. In order to verify the level density effect, the cross sections of the $^{186}W(\gamma,n)^{185}Ta$ reaction were calculated taking into account the six level density models, including three phenomenological models and three microscopic models [28–30], namely:
Constant temperature + Fermi gas (Ldmode 1),
Back-shifted Fermi gas (Ldmode 2),
Generalized superfluid (Ldmode 3),
Microscopic level densities (Skyrme force) from Goriely's tables (Ldmode 4),
Microscopic level densities (Skyrme force) from Hilaire's combinatorial tables (SFH) (Ldmode 5), and
Microscopic level densities (temperature dependent HFB, Gogny force) from Hilaire's combinatorial tables (Ldmode 6).

The gamma strength function used is the Brink-Axel Lorentzian model, which is often called the default model. The cross sections for the $^{186}W(\gamma,p)$ ^{185}Ta reaction, calculated using the TALYS-1.95 code [21], taking into account the six level density models (Ldmode1-Ldmode6) are shown in Fig. 4. In addition, in Fig. 4, we also plot the values of TENDL-2021 library [31] for comparison.

As can be seen in Fig. 4, the reaction cross sections calculated using the TALYS-1.95 code [21] considering six different level density models exhibit considerable dispersion. The cross section values peak at a photon energy of around 25 MeV, and the difference between the values calculated using different level density models can reach a factor of ~ 1.4. However, the difference between the cross section values at photon energies above 50 MeV is not significant, except for the cross section curve calculated using Ldmode 2. The comparison also indicates that the cross section curve from the TENDL-2021 library [31] overestimates all cross section curves

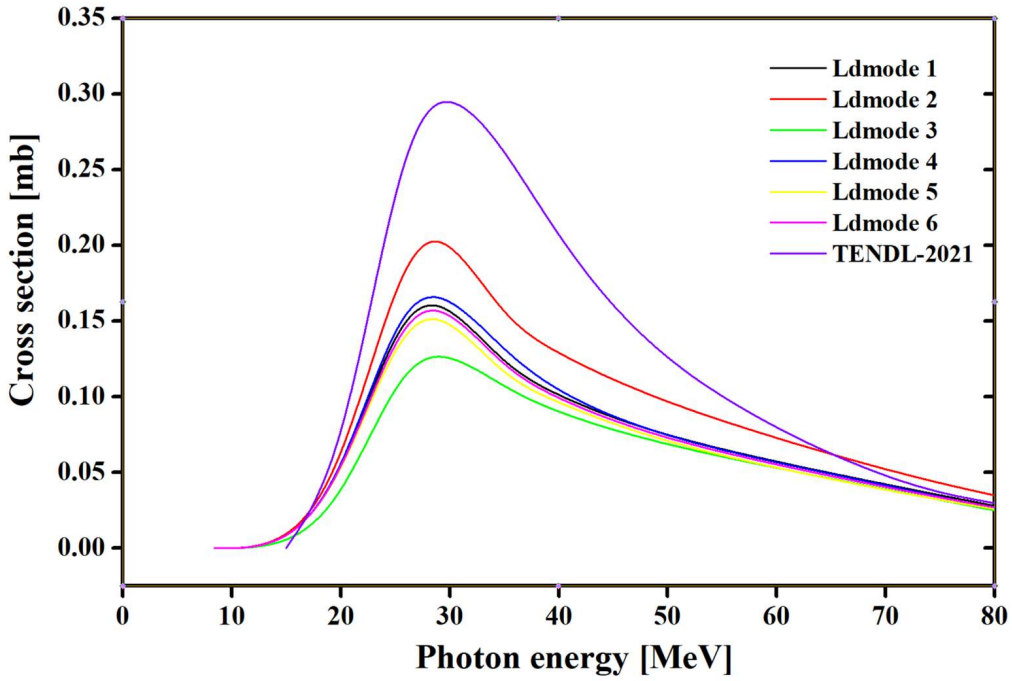

Fig. 4. (Color online) Energy dependent cross section of the ^{186}W$(\gamma, p)^{185}$Ta reaction, calculated using the TALYS-1.95 code, considering six level density models (Ldmode1-Ldmode6) and the theoretical data from the TENDL-2021 library [31].

calculated using the TALYS-1.95 code [21] with six level density models. Meanwhile, the cross section values of TENDL-2021 library [31] is lower than the evaluated values of ENDF/B-VII library [32]. The reason for this discrepancy may be due to the inconsistency of the level densities used.

Based on the energy-dependent cross sections calculated with six level density models using the nuclear model code TALYS-1.95 [21], we calculated the flux-weighted average cross sections for the ^{186}W$(\gamma, p)^{185}$Ta reaction. The measured and calculated flux-weighted average cross sections are given in Table 2, namely the experimental result is given in the third column and the theoretical results calculated using the six level density models (Ldmode 1-Ldmode 6) are given in the fourth to ninth columns. For better visualization, the measured and calculated results are also presented in Fig. 5.

As shown in Fig. 5, the results calculated using the six level density models differ significantly. Further comparison shows that only the result calculated with Ldmode 2 agrees with the experimental result, namely at the bremsstrahlung endpoint energy of 70 MeV the difference between the measured and calculated results is only about 4%. Meanwhile, all other calculation results differ significantly from the experimental result, in particular the calculated result with Ldmode 3 differs about 60% from the experimental result. This fact suggests that more experimental data on the ^{186}W$(\gamma, p)^{186}$Ta reaction are needed for comparison and verification of the level density model of ^{185}Ta.

Table 2. Measured and calculated flux-weighted average cross section of the $^{186}W(\gamma,p)^{185}Ta$ reaction at the bremsstrahlung end-point energy of 70 MeV.

Nuclear reaction	Bremss. end-point energy (MeV)	Flux-weighted average cross section (mb)						
		Experimental result	TALYS-1.95 calculation					
			Ldmode1	Ldmode2	Ldmod3	Ldmod4	Ldmod5	Ldmode6
$^{186}W(\gamma,p)^{185}Ta$	70	0.105 ± 0.011	0.078	0.101	0.065	0.081	0.075	0.076

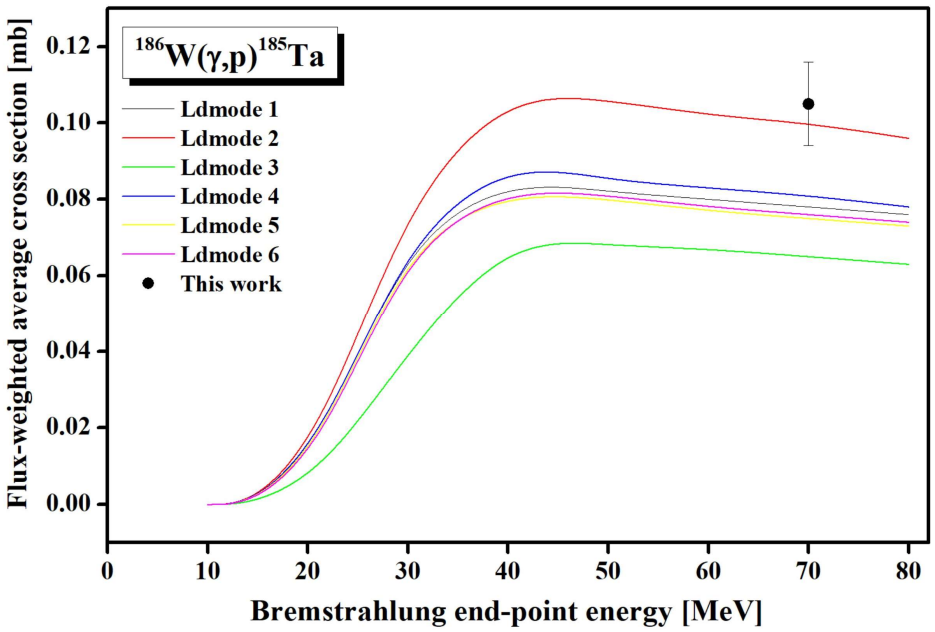

Fig. 5. (Color online) The measured and calculated flux-weighted average cross section of the $^{186}W(\gamma,p)^{185}Ta$ reaction. The calculations were carried out with the six different level density models (Ldmode 1- Ldmode 6).

4. Conclusion

The flux-weighted average cross section of the $^{186}W(\gamma,p)^{185}Ta$ reaction was measured at the bremsstrahlung end-point energy of 70 MeV. The measurement was carried out by the activation method in combination with off-line gamma spectrometry. Theoretical calculations were also carried out by incorporating the cross section values obtained from the TALYS 1.95 code and the bremsstrahlung flux simulated using the computer program MCNPX. When calculating the

reaction cross section, six level density models were considered and the results show that the flux-weighted average cross section of the $^{186}\mathrm{W}(\gamma, p)^{185}\mathrm{Ta}$ reaction calculated using Ldmode2 with the back-shifted Fermi gas model gives the best fit to the experimental result. The present result is published for the first time.

Acknowledgments

The authors would like to express their sincere thanks to the support of the Pohang Accelerator Laboratory (PAL) for carrying out the experiment and the laboratory staff for the excellent operation of the electron linac. Authors K. T. Thanh and T. D. Trong are grateful to the International Physics Center of the Institute of Physics, Vietnamese Academy of Science and Technology (VAST) for partial financial support, under Grant No. ICP.2023.10.

References

[1] A. Zilges, D. Balabanski, J. Isaak and N. Pietralla, *Photonuclear reactions—from basic research to applications*, Progress in Particle and Nuclear Physics **122** (2022) 103903.

[2] N. Pietralla, J. Isaak and V. Werner, *Photonuclear reactions: Achievements and perspectives*, Eur. Phys. J. A **55** (2019) 1.

[3] N. Van Do, N. T. Luan, N. T. Xuan, P. D. Khue, N. T. Hien, G. Kim *et al.*, *Measurement of yield ratios for the isomeric pair $^{137m,g}Ce$ in the $^{141}Pr(\gamma,x)^{137m,g}Ce$ reactions with bremsstrahlung end-point energies of 50-, 60-, and 70-MeV*, Radiat Phys. Chem. **176** (2020) 109016.

[4] P. Tkac, S. Chemerisov, R. Gromov, J. Song, J. Nolen, V. Makarashvili *et al.*, *Side-reaction products identified for photo-nuclear production of99mo*, J. Radioanal. Nucl. Chem. **326** (2020) 543.

[5] V. A. Zheltonozhsky and A. M. Savrasov, *Excitation of $^{179}Hf^{m2}$ with (γ,n)-reaction*, Nucl. Instr. Meth. B **456** (2019) 116.

[6] V. N. Starovoitova, P. L. Cole and T. L. Grimm, *Accelerator-based photoproduction of promising beta-emitters ^{67}Cu and ^{47}Sc*, J. Radioanal. Nucl. Chem. **305** (2015) 127.

[7] Y. Kavun and R. Makwana, *Study of (γ, p) reaction cross-section calculations of ^{52}Cr, ^{54}Fe, ^{60}Ni and ^{64}Zn isotopes*, Nucl. Instr. Meth. B **472** (2020) 72.

[8] Y. Kavun, S. Parashari and E. Tel, *Investigation of (γ, p) reaction cross-section calculations of ^{40}Ca, ^{70}Ge and ^{90}Zr isotopes*, Appl. Radiat. Isot. **164** (2020) 109318.

[9] S. Yang, K. Kim, G. Kim, H. Kim, Y. Lee, M. Lee *et al.*, *Measurement of isomeric yield ratio of $^{143m,g}Sm$ from $^{nat}Sm(\gamma,xn)$ reaction with end-point bremsstrahlung energies of 40-60 MeV*, Nucl. Data Sheets **119** (2014) 314.

[10] N. V. Do, N. T. Luan, N. T. Xuan, P. D. Khue, K. T. Thanh, B. V. Loat *et al.*, *Integrated cross sections of the photo-neutron reactions induced on ^{197}Au with 60 MeV bremsstrahlung*, Comm. Phys. **30** (2020) 49.

[11] N. V. Do, N. T. Luan, N. T. Xuan, K. T. Thanh, N. T. Hien and G. Kim, *Multiparticle $^{nat}Sr(\gamma,xnyp)$ reactions induced with bremsstrahlung end-point energies of 55, 60, and 65 MeV*, Chinese Phys. C **46** (2022) 094003.

[12] F. D. S. Butement, *New radioactive isotopes produced by nuclear photo-disintegration*, Nature **165** (1950) 149.

[13] T. Shizuma, T. Ishii, H. Makii, T. Hayakawa, S. Shigematsu, M. Matsuda *et al.*, *Evidence for a $k\pi = 1/2^+$ isomer in neutron-rich ^{185}Ta*, Eur. Phys. J. A **34** (2007) 1.

[14] Y. Li, F. Zhou, Y. Hao, X. Ma, P. Ji, X. Zhang *et al.*, *New cross section measurements on tungsten isotopes around 14 mev neutrons and their excitation functions*, Chinese Phys. C **46** (2022) 054003.

[15] G. Løvhøiden, D. G. Burke, E. R. Flynn and J. W. Sunier, *Single-proton states in ^{185}Ta studied with the $(\vec{\tau}, \alpha)$ reaction*, Phys. Scr. **22** (1980) 203.

[16] Semkova, V., Capote, R., Jaime Tornin, R., Koning, A. J., Moens, A. and Plompen, A. J.M., *New cross section measurements for neutron-induced reactions on Cr, Ni, Cu, Ta and W isotopes obtained with the activation technique*, Int. Conf. Nucl. Data Sci. Technol. (2007) 559.

[17] H. Sakane, M. Shibata, K. Kawade, Y. Kasugai and Y. Ikeda, *Systematics of (n, n'p) reaction cross sections by 14 mev neutron*, JAERI-Conf 2000-005 (2000) JP0050647.

[18] O. Deiev, I. Timchenko, S. Olejnik, V. Kushnir, V. Mytrochenko and S. Perezhogin, *Isomeric ratio of the* $^{181}Ta(\gamma,3n)^{178m,g}Ta$ *reaction products at energy e*γ_{max} *up to 95 MeV*, Chinese Phys. C **46** (2022) 014001.

[19] H. Naik, G. Kim, K. Kim, M. Zaman, A. Goswami, M. W. Lee *et al.*, *Measurement of flux-weighted average cross sections for* $^{197}Au\ (\gamma,xn)$ *reactions and isomeric yield ratios of* $^{196m,g}Au$ *with bremsstrahlung*, Nucl. Phys. A **948** (2016) 28.

[20] V. A. Zheltonozhsky and A. M. Savrasov, *Excitation of* $^{179}Hf^{m2}$ *with* (γ,n)*-reaction*, Nucl. Instr. Meth. B **456** (2019) 116.

[21] A. Koning and D. Rochman, *Modern nuclear data evaluation with the TALYS code system*, Nucl. Data Sheets **113** (2012) 2841.

[22] E. N. R. Data, *National Nuclear Data Center*, 2000.

[23] N. Do, P. Khue, K. Thanh, T. Nam, M. Rahman, K.-S. Kim *et al.*, *Measurement of isomeric yield ratios for the* $^{44m,g}Sc$ *isomeric pairs produced from* ^{45}Sc *and* ^{nat}Ti *targets at 50-, 60-, and 70-MeV bremsstrahlung*, J. Radioanal. Nucl. Chem. **287** (2011) 813.

[24] V. Di Napoli, A. Lacerenza, F. Salvetti, H. De Carvalho and J. B. Martins, *Production of* ^{24}Na *and* ^{22}Na *from* ^{27}Al *by high-energy photons*, Lett. al Nuovo Cimento (1971-1985) **1** (1971) 835.

[25] J. S. Hendricks, W. M. Gregg, L. F. Michael, R. J. Michael, C. J. Russell, W. D. Joe *et al.* tech. rep.

[26] V. D. Nguyen, D. K. Pham, T. T. Kim, D. T. Tran, V. D. Phung, Y. S. Lee *et al.*, *Measurement of isomeric cross-section ratios for the* $^{45}Sc,\ (\gamma,n)^{44m,g}Sc,\ ^{nat}Ti\ (\gamma,x)^{44m,g}Sc,\ ^{103}Rh(\gamma,4n)^{99m,g}Rh,$ *and* $^{nat}Fe(\gamma,x)^{52m,g}Mn$ *reactions induced by 65-MeV bremsstrahlung*, Journal of the Korean Physical Society **50** (2007) 417.

[27] R. Capote, M. Herman, P. Obložinský, P. Young, S. Goriely, T. Belgya *et al.*, *Ripl – reference input parameter library for calculation of nuclear reactions and nuclear data evaluations*, Nucl. Data Sheets **110** (2009) 3107.

[28] M. Arnould and S. Goriely, *Microscopic nuclear models for astrophysics: The brussels bruslib nuclear library and beyond*, Nucl. Phys. A **777** (2006) 157.

[29] S. Hilaire and S. Goriely, *Global microscopic nuclear level densities within the hfb plus combinatorial method for practical applications*, Nucl. Phys. A **779** (2006) 63.

[30] A. J. Koning, S. Hilaire and S. Goriely, *Global and local level density models*, Nucl. Phys. A **810** (2008) 13.

[31] TENDL-2021, *Talys-based evaluated nuclear data library*, Nuclear Research and Consultancy Group (Available at `https://tendl.web.psi.ch/tendl_2021/tendl2021.html`) .

[32] IAEA, *Evaluatead nuclear data file (ENDF)*, Data Version of 2023-08-25 (Available at `https://www.iaea.org/resources/databases/evaluated-nuclear-data-file`) .